

Collective behavior of evaporating droplets on superhydrophobic surfaces

AIChE Journal

Moradi Mehr, Shiva; Businaro, Luca; Habibi, Mehdi; Moradi, Ali Reza

<https://doi.org/10.1002/aic.16284>

This publication is made publicly available in the institutional repository of Wageningen University and Research, under the terms of article 25fa of the Dutch Copyright Act, also known as the Amendment Taverne. This has been done with explicit consent by the author.



Article 25fa states that the author of a short scientific work funded either wholly or partially by Dutch public funds is entitled to make that work publicly available for no consideration following a reasonable period of time after the work was first published, provided that clear reference is made to the source of the first publication of the work.

This publication is distributed under The Association of Universities in the Netherlands (VSNU) 'Article 25fa implementation' project. In this project research outputs of researchers employed by Dutch Universities that comply with the legal requirements of Article 25fa of the Dutch Copyright Act are distributed online and free of cost or other barriers in institutional repositories. Research outputs are distributed six months after their first online publication in the original published version and with proper attribution to the source of the original publication.

You are permitted to download and use the publication for personal purposes. All rights remain with the author(s) and / or copyright owner(s) of this work. Any use of the publication or parts of it other than authorised under article 25fa of the Dutch Copyright act is prohibited. Wageningen University & Research and the author(s) of this publication shall not be held responsible or liable for any damages resulting from your (re)use of this publication.

For questions regarding the public availability of this publication please contact openscience.library@wur.nl

Collective behavior of evaporating droplets on superhydrophobic surfaces

Shiva Moradi Mehr¹ | Luca Businaro² | Mehdi Habibi³  | Ali-Reza Moradi^{1,4} 

¹Department of Physics, Institute for Advanced Studies in Basic Sciences (IASBS), Zanjan, 45195-1159, Iran

²Italian National Research Council - Institute for Photonics and Nanotechnologies (CNR - IFN), Rome, Italy

³Physics and Physical Chemistry of Foods, Wageningen University, 6700 AA Wageningen, The Netherlands

⁴School of Nano Science, Institute for Research in Fundamental Sciences (IPM), Tehran 19395, 19395-5531, Iran

Correspondence

Ali-Reza Moradi, Department of Physics, Institute for Advanced Studies in Basic Sciences, Zanjan, 45195-1159, Iran.
Email: moradika@iasbs.ac.ir

Abstract

We study the evaporation dynamics of multiple water droplets deposited in ordered arrays or randomly distributed (sprayed) on superhydrophobic substrates (SHP) and smooth silicon wafers (SW). The evaluation of mass of the droplets as a function of time shows a power-law behavior with exponent 3/2, and from the prefactor of the power-law an evaporation rate can be determined. We find that the evaporation rate on a SHP surface is slower than a normal surface for both single droplet and collection of droplets. By dividing a large droplet into more smaller ones, the evaporation rate increases and the difference between the evaporation rates on SHP and SW surfaces becomes higher. The evaporation rates depend also on the distance of the droplets which increase with increasing this distance.

KEYWORDS

collective behavior, droplets, superhydrophobic surface, water evaporation

1 | INTRODUCTION

The evaporation of a water droplet is a common phenomenon in nature and has significant applications in technology (e.g., ink-jet printing and surface patterning),^{1,2} biology (e.g., bio-sensing and micro-fluidics),³⁻⁵ and environmental science (e.g., cooling effect of increased evaporation from trees on the global climate).⁶⁻⁸ Therefore, it has been subject of intense scientific studies in the recent years.⁹⁻¹⁴ In order to achieve a full picture of the evaporation mechanism many characteristic aspects of it have to be investigated, such as the evaporation rate, flow pattern inside the droplet, air flow, humidity conditions, properties of the surface and so forth. Picknett and Bexon identified two modes of evaporation for evaporation of a water droplet on a smooth surface; the constant contact angle (CCA) mode and the constant contact line (CCL) mode.¹⁵ In general, the evaporation of a single droplet can exhibit a mixed evaporation behavior, often denoted by stick-sliding mode. In CCL mode, the initial contact line remains constant and the contact angle slowly decreases with time. For the CCA mode, the contact line decreases at the fixed contact angle. Dynamics of droplet evaporation clearly depends on the droplet contact angle therefore, hydrophobicity, contact angle hysteresis, and surface roughness play roles in the evaporation dynamics.¹⁶ Contact

line dynamics and wetting transition during evaporation of a single water droplet on a superhydrophobic (SHP) substrate is also investigated in details.^{13,17} It is shown that the higher contact angle of droplet may change the evaporation modes at various stages of the process.¹⁶ In many industrial or environmental applications the evaporation occurs in the presence of other droplets. It is recently shown that the evaporation of a collection of droplets on a normal surface is significantly different from single droplet evaporation due to the collective effects.¹⁰ The justification is that the surroundings of each droplet are partially saturated by the vapor from the other ones leading to slower evaporation rate. This collective dynamics in evaporation and overlap of evaporation flux has been studied through a model in which the collection of the droplets has been considered as a superdroplet with the radius obtained from the area covered by the small droplets.¹⁰ In this view, the collective dynamics of multiple droplets evaporating on a SHP surface requires a special attention as it has not been investigated. In this study, we investigate the evaporation dynamics of ordered arrays of mono-dispersed and sprayed droplets on SHP and silicon wafer (SW, as a normal substrate) surface to consider the collective behavior of evaporation. We also perform single droplet evaporation experiments on both substrates as controlled experiments. To this aim we change the droplet size, distance

between the droplets and size distribution of sprayed droplets. We also investigate the morphology of droplets during the evaporation and investigate the evaporation rate for droplets deposited at the edges of an array. Our results might be important for designing self-cleaning surfaces or arrays of droplets for biomedical applications and even environmental applications such as controlling the evaporation rate.

2 | MATERIALS AND METHODS

We use an artificial rough micro-fabricated surface called biomimetic SHP surface. The SHP substrate are fabricated on a 100 SW by electron beam lithography (Vistec EPBG-5HR acceleration voltage: 100 keV) and Inductive Coupled Plasma (ICP) Si etching. A 1.2 μm thick layer of Shipley UVIII electronic resist is spun on the silicon surface, expose with a dose of 25 $\mu\text{C}/\text{cm}^2$ and developed. A thin Cr film (30 nm thickness) is then deposited and lifted off to define the device pattern, which is an array of pillars of 5 μm side and 14 μm pitch. The device pattern is transferred on the substrate by a two-steps ICP Si etching; In the first step (protection), the parameters are kept as pressure = 100 mTorr, Ar = 30 sccm, C4F8 = 187 sccm, ICP = 600 W, $t = 2$ s, and in the second step (etching), as pressure = 100 mTorr, Ar = 100 sccm, SF6 = 90 sccm, cathode bias = 70 V, ICP = 500 W, $t = 10$ s. As for the saw-shaped pillars array, a 400 nm thick layer PMMA 950 K 9% is spun on a SW, expose with a dose of 700 $\mu\text{C}/\text{cm}^2$ and developed. A 30 nm thick Cr film is then deposited by e-gun assisted evaporator and lifted off. The device pattern is transferred on the substrate by the same ICP etching procedure. After cleaning in Piranha solution ($\text{H}_2\text{SO}_4/\text{H}_2\text{O}_2 = 3:1$), both microstructured SWs are salinized to impart the SHP behavior with 10% trimethylchlorosilane in toluene. The resulting surface show a contact angle for DI water $\theta > 150^\circ$ and a roll off angle $< 4^\circ$. The SHP areas are fabricated in four different zones of 6 mm \times 6 mm distanced by 4 mm from each other.

The rest of the silicone surface remain unpatterned and is used as a normal substrate in comparative study. In Figure 1a a SEM tilted image (52°) along with its magnified view of the fabricated sample is shown. Various configurations of water droplets are made on SHP and SW surfaces (Figure 1b–e) by using a micro-syringe. In the first series of experiments the initial total volume of the liquid deposited on the surface is 40 μl . We deposit this amount as a single drop of 40 μl or different combinations of smaller mono-dispersed droplets in form of arrays: two 20 μl , four 10 μl , eight 5 μl and sixteen 2.5 μl as shown in Figure 1b–e. The experiments are within the limit of slow and quasi-steady evaporation, by keeping the temperature of the system at 22°C throughout the experiments. The experiments are performed on both SHP and smooth SW surfaces in a humidity controlled chamber at a humidity of 50%. The droplet mass variation during the evaporation is measured using a weighting balance (Sartorius, BL 120S) with accuracy of 10^{-4} g. Evolution of the shape of the droplets are captured in some of the experiments by video imaging (DCC1545M, Thorlabs, 8 bit dynamic range, 5.2 μm pixel pitch, at 10 s time intervals). The morphometric parameters of the droplets are measured using image processing of the video sequences. These parameters are defined in the schematic view of the droplet in Figure 1f. For spray experiments we use a metal fine spray nozzle with minimum drop diameter of about 30 μm . Two different distances of 15 and 30 cm between the nozzle and the substrate with different number of puffs are used to achieve different droplet distributions. The SW areas are covered by a mask during the mass measurement in the spray experiments.

3 | EXPERIMENTAL RESULTS AND DISCUSSION

By acquisition of video images from the side view of the evaporating droplets and follow-up image analysis, morphometric parameters such

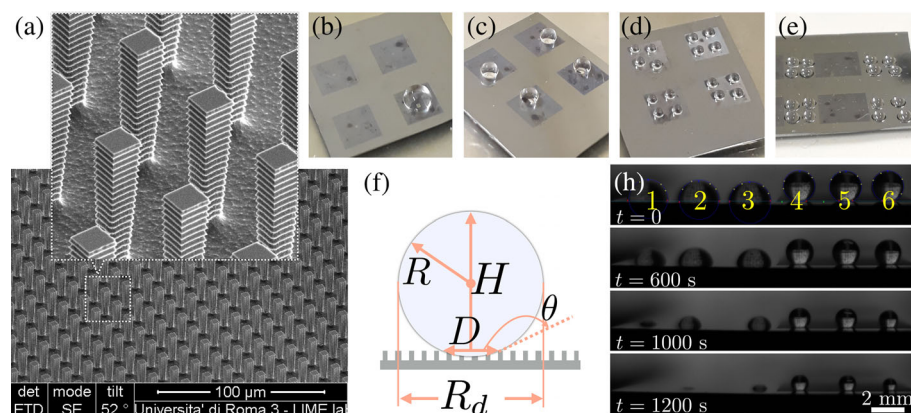


FIGURE 1 (a) A SEM tilted image (52°) and its magnified view of the SHP substrate; (b–e) The various collection of water droplets of equivalent total mass on the SHP and SW surfaces: (b) 1 droplet of 40 μl , (c) 4 droplets of 10 μl and (d) 16 droplets of 2.5 μl on SHP surface; (e) 16 droplets of 2.5 μl on SW surface; (f) Definition of droplet parameters; (g) Side view of droplets on SW and SHP substrates to compute morphometric information of droplets in time. SHP, superhydrophobic; SW, silicon wafers [Color figure can be viewed at wileyonlinelibrary.com]

as contact angle and diameter of contact area can be extracted. In Figure 2 the time evolution of the contact angle, the contact line, and the height of the six droplets of Figure 1g is shown. The image analysis is performed in MATLAB® by finding the best fitted circle to the 2D images of the side view of the droplets. Data are calculated with a time resolution of 10 s. The evaporation on the both SHP and SW surfaces occurs mainly in CCA mode. The contact angle for the SHP case is $157^\circ \pm 4^\circ$ and for SW surface is $89^\circ \pm 4^\circ$. Only close to vanishing of the droplet the contact angle reduces abruptly to about zero. The abrupt transition to zero degree could be attributed to the Cassie-to-Wenzel transition, which occurs when Laplace pressure increases at small droplet volume.¹⁸ Diameter of the contact area (D) decreases monotonically to evaporate droplets on the normal surface. This indicates that the contact line is not pinned and moves as long as the contact angle is fixed. As it is clear from Figure 2b, the evaporation rate for Droplet 1 is higher than Droplet 2 and 3 (Figure 1g) and D of Droplet 1 reaches to zero faster than that of the other two. The same behavior is also observed for the height (H) of this droplet (Figure 2c). This is due to the fact that Droplet 1 is at the edge of the array while the other two are in between the other droplets. Due to the edge effects the evaporation flux from this droplet is not symmetric and there is a larger flux of evaporation toward the left side of the droplet. In contrast to the SW case, D for the drops on SHP surfaces is roughly constant during evaporation. It shows very slight decrease close to the end and goes sharply to zero. It has been previously shown that in the evaporation of a single droplet on a SHP surface, the contact line shrinks at a much slower rate.¹⁷ On SHP substrates, all evaporation modes may occur; the CCA mode is mostly observed when the contact angle hysteresis is low.¹⁹ D behaves roughly the same for the three droplets on the SHP surface (Droplets 4, 5 and 6 in Figure 1g). Even for Droplet 6 deposited at the other edge of the array, D is the same as the other two, however the height (H) of Droplet 6 decreases faster than the other two droplets for the same reason as explained above for Droplet 1.

Figure 3a summarizes the time evolution of mass of various collections of droplets evaporation on SHP and SW surfaces in a log-lin

scale. Since all the collections have the same initial total mass of 40 mgr all the curves start from this point at time zero. We know that for a small droplet, volume (V) scales as R^3 , R being the radius of the droplet, and from $\frac{dV}{dt} \propto R$,^{9,10,20} it follows that $R \propto (t_f - t)^{1/2}$, where t_f is the total evaporation time. Therefore, it is expected that mass of the droplet changes in power-law in time with an exponent 3/2 as: $m = A(t_f - t)^{3/2}$. The experimental results confirm 3/2 scaling power for different collections of droplets. Small deviation from the above scaling can be observed at the end of the process. This is mainly due to the fact that the droplets at the edge of the array evaporate faster and vanish before the other droplets, therefore they do not contribute in the final evaporation data. By fitting the above function to our data (solid lines) the pre-factor A for different collections of droplets can be determined. It is known that the pre-factor A depends on the vapor concentration and diffusion coefficient in the atmosphere, the contact line of the droplet, and the density of the liquid.^{20,21} Figure 3b shows the pre-factor A obtained by fitting the data as a function of inverse of the number of droplets in the collection ($1/N$). The measured pre-factor A is higher on SW surface than SHP surface which means the evaporation on SHP surfaces is slower than the evaporation on SW surfaces. This can be confirmed by looking at the total evaporation time (Figure 3c). In these experiments, we observe that A increases with up to 3 (2) folds by increasing the number of droplets in the array for the SW (SHP) substrate. Therefore, a collection of small droplets evaporates faster than a single droplet with the same initial mass which is in agreements with previous studies.^{9,10} This effect is more pronounced for evaporation on the SW surface with respect to SHP surface as shown in Figure 3c. The main reason for increasing the evaporation rate by reducing the droplet size is due to increasing the total perimeter of the droplets, since the evaporation rate is proportional to the perimeter of the droplet.⁹ However, when the droplets are in closer vicinity of each other, their evaporation flux can overlap and they may partially saturate their surroundings. On the other hand, when the droplets are far away from each other, the influence of their vapor flux on the surrounding droplets suppress and results in faster

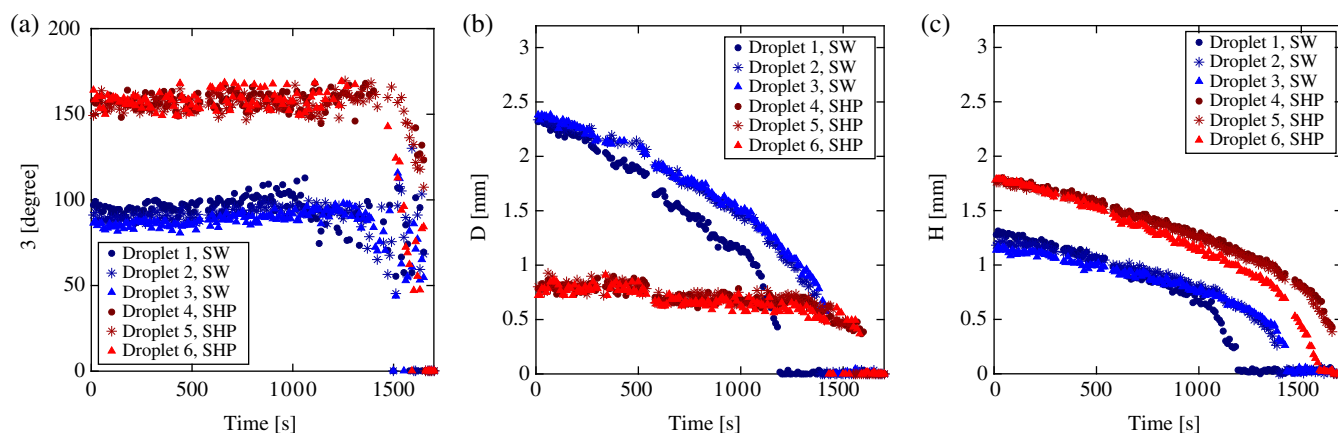


FIGURE 2 Image processing results; time evolution of (a) contact angle, (b) contact line, and (c) height of the six droplets shown in Figure 1e, positioned on SW surface (Droplets 1, 2, 3) and SHP surface (Droplets 4, 5, 6). SHP, superhydrophobic; SW, silicon wafers [Color figure can be viewed at wileyonlinelibrary.com]

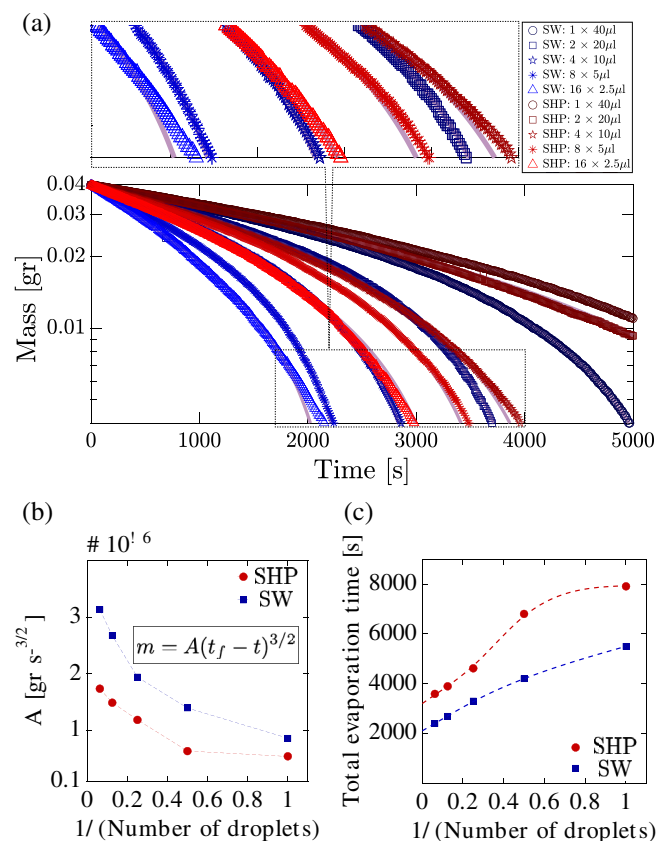


FIGURE 3 (a) Mass as a function of time during the evaporation of various sets of droplets on SHP and SW surfaces; (b) The two-third power fitting pre-factor (A) as a function of inverse of the number of droplets ($1/N$); (c) Total evaporation time as a function of $1/N$. SHP, superhydrophobic; SW, silicon wafers [Color figure can be viewed at wileyonlinelibrary.com]

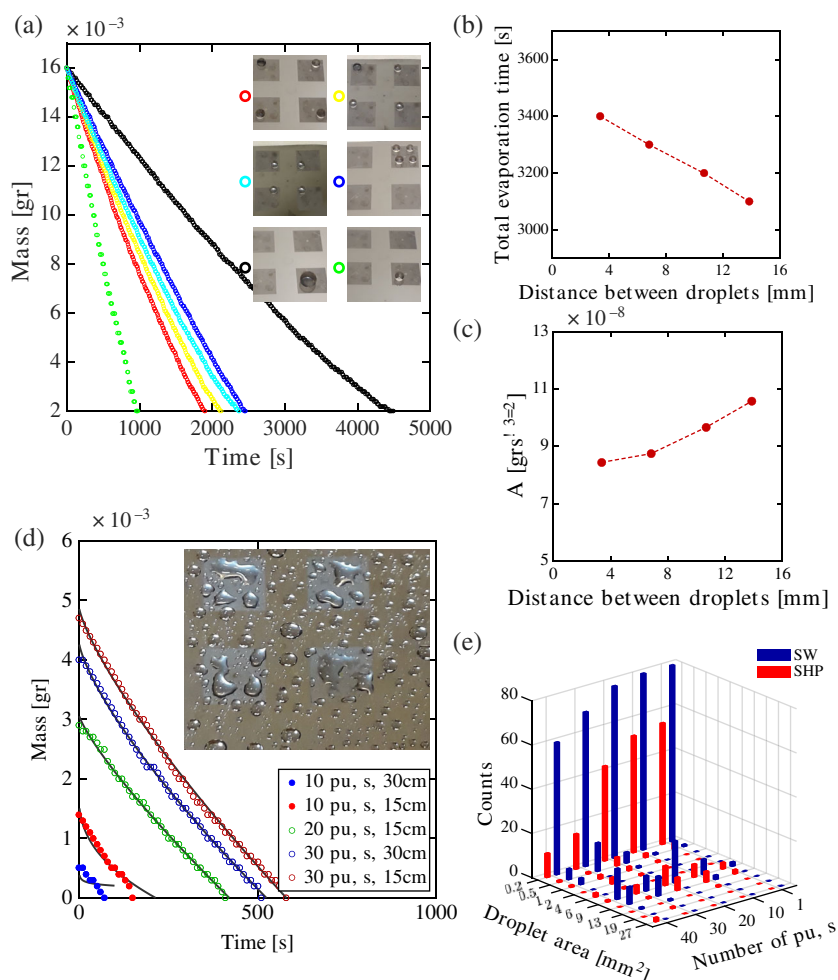
evaporation. Therefore, the distance between droplets in an array plays an important role on the evaporation dynamics since this distance determines how the evaporation flux can be overlapped. The effect of the distance between droplets in an array on the evaporation rate is demonstrated in Figure 4a. In this graph, the mass of droplets is shown as a function of time for six sets of evaporation on a SHP surface. The total initial volume of droplets for all experiments is 16 μl except the experiments shown by green symbol. The black and green symbols are representing single droplet experiments for 16 and 4 μl droplets, respectively. The mass data for green symbols are multiplied by four to represent four droplets of 4 μl deposited at infinite distance. The single droplet experiments are performed as controlled experiments and show the slowest (for the 16 μl single droplet) and fastest (for the 4 μl single droplet) evaporation rates. The other four data sets representing the evaporation of four droplets of 4 μl deposited at a center to center distance of 3.4, 6.8, 10.7, and 13.9 mm for dark blue, light blue, yellow and red symbols, respectively, as shown in the inset of Figure 4a. The maximum time for evaporation decrease monotonically by increasing the center to center distance between the droplets as shown in Figure 4b. In addition the parameter A can be determined by fitting 3/2 power-law relation to the data. This

parameter represents the evaporation rate and increases by increasing the distance (Figure 4c). The highest evaporation rate can be achieved when the four droplets are deposited at infinite distance (green symbols in Figure 4a).

In many real life applications both in technology (e.g., spraying) and nature (e.g., raining) the droplets are distributed with random sizes and distances on a surface. While spraying a liquid, different parameters such as the pressure and geometry of the nozzle, and viscosity and surface tension of the liquid determine the droplet shape and size distribution²² and consequently affect the evaporation dynamics. The collective dynamics of sprayed droplets on normal surfaces (contact angle $\approx 90^\circ$) have been studied by Carrier et al¹⁰ and it is shown that for widely differing size distribution the total mass as a function of time scales like an exponential. To study how the collective dynamics of droplets with random size distribution effect on the evaporation, we also measure evolution of the total mass in time (Figure 4d). We change the distance from the nozzle to the surface and number of puffs which results in different size distributions (Figure 4e) and initial mass of the droplets on the surface. As expected, by spraying from closer distances or spraying more puffs the larger droplets are deposited on the surface. With respect to SW substrate larger droplets are formed on SHP substrates at similar spraying conditions, as shown in the image of the inset of Figure 4d. Nevertheless, our experiments demonstrate that the evaporation behavior on SHP surfaces follows a similar exponential trend to the SW surfaces, except in the cases of less puffs from longer spray distances, such as the one shown by filled blue symbols in Figure 4d. The deviation from the exponential trend that is observed mainly for 10 puffs experiments is due to the fact that the size distribution of these experiments deviates from a random distribution.

Along with technological applications of SHP surfaces for anti-wetting and self-cleaning materials,^{23,24} they have attracted a large interest in recent years to investigate whether they can be exploited to study biological systems.²⁵⁻²⁷ SHP surfaces are very promising in terms of actual applicability to clinical practice, nevertheless, researchers have considered them also for more fundamental issues, such as optimizing the surface features with the aim of precisely controlling the wetting and dewetting phenomena at the interface between liquids and solids. In modern biomedicine, SHP surfaces have been incorporated in ultrasensitive biosensors to detect molecular markers,²⁸ smart drug delivery systems,²⁹ and DNA decondensation,³⁰ to name a few. In Reference 28, the superhydrophobicity behavior has been used to enhance the sensitivity of FTIR biosensors toward enabling them for a label-free and non-destructive detection down to the femtomole concentration range, of analytes in diluted solutions, for example, ferritin, which is a blood protein and is a relevant parameter for the early detection of Alzheimer's disease. In Reference 29, smart implantable drug delivery systems based on SHP 3D meshes have been proposed for controlled drug release in long-term treatment, and in Reference 30, the usefulness of SHP surfaces in controlling the de-wetting dynamics of droplet containing genomic DNA toward fabrication of a large ordered robust-configurations of stretched DNA filaments and nanometric

FIGURE 4 (a) The mass of different arrangements of droplets with the same initial mass on a SHP surface as a function of time; (b) The total evaporation time and (c) two-third power fitting pre-factor as a function of the distance between droplets; (d) Total mass as a function of time during the evaporation of sprayed droplets on SHP substrate for various distances and number of puffs. For 10 puffs experiments due to the fact that the size distribution of these experiments deviates from a random distribution a significant deviation from the exponential trend is observed; (e) Size distribution of the droplets sprayed from 30 cm for different number of puffs. SHP, superhydrophobic [Color figure can be viewed at wileyonlinelibrary.com]



controlling of their position and orientation is demonstrated. DNA decondensation is crucial for its visualization, which, in turn, is useful in the development of novel DNA chips for genetic analysis in molecular biology and health sciences. The presented results on the collective behavior of evaporating droplets on SHP might provide insight for the applications related to the aforementioned classes, as evaporating droplets always play a role in such applications.

4 | CONCLUSION

We investigated experimentally the evaporation dynamics of collection of droplets (randomly distributed and ordered arrays) on SHP surfaces. The results were compared with single droplet evaporation. By tracking the temporal evolution of droplets mass and morphometric video imaging the following conclusions have been drawn from this study:

- For evaporation on a SHP surface the contact area and contact angle of the droplets are constant until the droplet becomes very small. We found that a collection of smaller droplets deposited in

an array evaporate faster compared to a single droplet with the same total initial mass, due to increasing the effective perimeter of droplets which provides higher evaporation flux.

- Having another droplet in the neighborhood can decrease the evaporation rate due to overlap of evaporation fluxes. Therefore, increasing the distances between the droplets in an array can increase the evaporation rate by reducing the overlap of the evaporation fluxes.
- In an array of droplets the droplets at the edges evaporate faster due to non-uniform evaporation fluxes which is larger at the empty sides.
- For random distribution of droplets on a SHP surface achieved by spraying from various distances or spraying different numbers of puffs our experiments demonstrate that the evaporation behavior follows a similar trend in all cases in alignment with the results of ordered arrays of droplets.
- Our results indicate that the collective evaporation rate on a SHP substrate is in general lower than that of a normal substrate. These results might provide insight for designing self-cleaning surfaces or droplet arrays for modern biomedicine, photonics, and technological applications as well as in managing under-evaporation water bodies.

ACKNOWLEDGMENTS

S. M. M. and A. M. thank Mohammad A. Charsooghi, Maniya Maleki, and Saeid Mollaei for useful discussions. The authors would like to thank Solmaz Moradi Mehr for editing the paper from the English language point of view.

NOTATION

SHP superhydrophobic

SW silicon wafer

ORCID

Mehdi Habibi  <https://orcid.org/0000-0003-4672-0516>

Ali-Reza Moradi  <https://orcid.org/0000-0002-4677-5800>

REFERENCES

1. Lim T, Han S, Chung J, Chung JT, Ko S, Grigoropoulos CP. Experimental study on spreading and evaporation of inkjet printed pico-liter droplet on a heated substrate. *Int J Heat Mass Transf.* 2009;52(1-2):431-441.
2. Adachi E, Dimitrov AS, Nagayama K. Stripe patterns formed on a glass surface during droplet evaporation. *Langmuir.* 1995;11(4):1057-1060.
3. Trantum JR, Baglia ML, Eagleton ZE, Mernaugh RL, Haselton FR. Biosensor design based on Marangoni flow in an evaporating drop. *Lab Chip.* 2014;14(2):315-324.
4. Cho SK, Moon H, Kim CJ. Creating, transporting, cutting, and merging liquid droplets by electrowetting-based actuation for digital microfluidic circuits. *J Microelectromech Syst.* 2003;12(1):70-80.
5. Javadi A, Habibi M, Taheri FS, Moulinet S, Bonn D. Effect of wetting on capillary pumping in microchannels. *Sci Rep.* 2013;3(1):1-6.
6. Morton FI. Evaporation research—a critical review and its lessons for the environmental sciences. *Crit Rev Environ Sci Technol.* 1994;24(3):237-280.
7. Tanny J, Cohen S, Berger D, et al. Evaporation from a reservoir with fluctuating water level: correcting for limited fetch. *J Hydrol.* 2011;404(3-4):146-156.
8. Ban-Weiss GA, Bala G, Cao L, Pongratz J, Caldeira K. Climate forcing and response to idealized changes in surface latent and sensible heat. *Environ Res Lett.* 2011;6(3):034032.
9. Shahidzadeh-Bonn N, Rafai S, Azouni A, Bonn D. Evaporating droplets. *J Fluid Mech.* 2006;549:307-313.
10. Carrier O, Shahidzadeh-Bonn N, Zargar R, et al. Evaporation of water: evaporation rate and collective effects. *J Fluid Mech.* 2016;798:774-786.
11. Habibi M, Moller P, Fall A, Rafai S, Bonn D. Pattern formation by dewetting and evaporating sedimenting suspensions. *Soft Matter.* 2012;8(17):4682-4686.
12. Popov YO. Evaporative deposition patterns: spatial dimensions of the deposit. *Phys Rev E.* 2005;71(3):036313.
13. Chen X, Ma R, Li J, et al. Evaporation of droplets on superhydrophobic surfaces: surface roughness and small droplet size effects. *Phys Rev Lett.* 2012;109(11):116101.
14. Devlin NR, Loehr K, Harris MT. The importance of gravity in droplet evaporation: a comparison of pendant and sessile drop evaporation with particles. *AIChE J.* 2016 Mar;62(3):947-955.
15. Picknett RG, Bexon R. The evaporation of sessile or pendant drops in still air. *J Colloid Interface Sci.* 1977;61(2):336-350.
16. McHale G, Aqil S, Shirtcliffe NJ, Newton MI, Erbil HY. Analysis of droplet evaporation on a superhydrophobic surface. *Langmuir.* 2005;21(24):11053-11060.
17. Gelderblom H, Marin AG, Nair H, et al. How water droplets evaporate on a superhydrophobic substrate. *Phys Rev E.* 2011;83(2):026306.
18. Liu G, Fu L, Rode AV, Craig VS. Water droplet motion control on superhydrophobic surfaces: exploiting the Wenzel-to-Cassie transition. *Langmuir.* 2011;27(6):2595-2600.
19. Kulinich SA, Farzaneh M. Effect of contact angle hysteresis on water droplet evaporation from super-hydrophobic surfaces. *Appl Surf Sci.* 2009;255(7):4056-4060.
20. Hwang IG, Kim JY, Weon BM. Droplet evaporation with complexity of evaporation modes. *Appl Phys Lett.* 2017;110(3):031602.
21. Stauber JM, Wilson SK, Duffy BR, Sefiane K. Evaporation of droplets on strongly hydrophobic substrates. *Langmuir.* 2015;31(12):3653-3660.
22. Kooij S, Sijs R, Denn MM, Villermaux E, Bonn D. What determines the drop size in sprays? *Phys Rev X.* 2018;8(3):031019.
23. Ueda E, Levkin PA. Emerging applications of superhydrophilic-superhydrophobic micropatterns. *Adv Mater.* 2013;25(9):1234-1247.
24. Nosonovsky M, Bhushan B. Superhydrophobic surfaces and emerging applications: non-adhesion, energy, green engineering. *Curr Opin Colloid Interface Sci.* 2009;14(4):270-280.
25. Ciasca G, Papi M, Businaro L, et al. Recent advances in superhydrophobic surfaces and their relevance to biology and medicine. *Bioinspir Biomim.* 2016;11(1):011001.
26. Lima AC, Mano JF. Micro-/nano-structured superhydrophobic surfaces in the biomedical field: part I: basic concepts and biomimetic approaches. *Nanomedicine.* 2015;10(1):103-119.
27. Lima AC, Mano JF. Micro-/nano-structured superhydrophobic surfaces in the biomedical field: part II: applications overview. *Nanomedicine.* 2015;10(2):271-297.
28. De Ninno A, Ciasca G, Gerardino A, et al. An integrated superhydrophobic-plasmonic biosensor for mid-infrared protein detection at the femtomole level. *Phys Chem Chem Phys.* 2015;17(33):21337-21342.
29. Yohe ST, Colson YL, Grinstaff MW. Superhydrophobic materials for tunable drug release: using displacement of air to control delivery rates. *J Am Chem Soc.* 2012;134(4):2016-2019.
30. Ciasca G, Businaro L, Papi M, et al. Self-assembling of large ordered DNA arrays using superhydrophobic patterned surfaces. *Nanotechnology.* 2013;24(49):495302.

How to cite this article: Moradi Mehr S, Businaro L, Habibi M, Moradi A-R. Collective behavior of evaporating droplets on superhydrophobic surfaces. *AIChE J.* 2020;e16284. <https://doi.org/10.1002/aic.16284>